KURENAI 紅
Kyoto University Research Information Repository

KYOTO UNIVERSITY

Title	<Original>Three Dimensional Analysis of Elastic Constants of the Wood Cell Wall
Author(s)	WATANABE, Ugai; NORIMOTO, Misato
Citation	Wood research : bulletin of the Wood Research Institute Kyoto University (2000), 87: 1-7
Issue Date	2000-09-30
URL	http://hdl.handle.net/2433/53153
Right	
Type	Departmental Bulletin Paper
Textversion	publisher

Three Dimensional Analysis of Elastic Constants
of the Wood Cell Wall

Ugai Watanabe[*1,2] and Misato Norimoto[*1]

(Received May 31, 2000)

Abstract——The elastic constants of wood cell wall were theoretically analyzed using two cell wall unit models and three sets of elastic constants for lignin-hemicellulose matrix. The Young's modulus of the cell wall layers in the direction perpendicular to the microfibril orientation increased remarkably with increasing Young's modulus and shear modulus of the matrix, although that in the microfibril direction didn't change significantly. The Young's modulus and shear modulus of the cell wall layers differed between the models depending on the volume fraction of cellulose and the presence of non-crystalline cellulose. The decrease in the longitudinal Young's modulus of the cell wall with the S_2 microfibril angle became more gentle with increasing Young's modulus and shear modulus of the matrix. A comparison between calculated and experimental results indicated that the wood cell wall would contain a non-crystalline cellulose with lower elastic moduli than crystalline cellulose and the Young's modulus of the lignin-hemicellulose matrix is at least more than 2 GPa.

Keywords: wood cell wall models, three dimensional analysis, elastic constants, non-crystalline cellulose, matrix

1. Introduction

The mechanical properties and their anisotropy of wood relate strongly to structure from the molecular to macroscopic levels. The elastic constants of the wood cell wall which depend on its composite and layered structures are important factors in the mechanical properties of whole wood. Generally, direct measurement of the elastic constants of the wood cell wall is very difficult, although an attempt to observe the elastic behavior of the wood cell wall has been made[1,2]. Therefore, the cell wall elastic constants have been estimated theoretically using cell wall models.

Cellulose, hemicellulose and lignin are the main chemical components affecting the elastic properties of wood. Tang et al.[3] and Ohgama et al.[4] evaluated theoretically the elastic constants of the cell wall using a unit model of the cell wall layer where a rigid framework mainly composed of crystalline cellulose was embedded in a lignin-hemicellulose matrix. In this simple model which contains all the cell wall layers, the essential structure of the real cell wall is taken into account. Norimoto et al.[5] proposed a more real cell wall unit model made up of three phases, namely, crystalline cellulose, non-crystalline cellulose and lignin-hemicellulose matrix to investigate the relationship between water adsorption and amorphous structure in the cell wall. For the Young's modulus of matrix substance, 2 or 4 GPa as the Young's modulus of lignin[6,7] has been adopted to calculate the cell wall elastic constants. Cousins[8] obtained an experimental value of about 8 GPa for hemicellulose which contains xylan and glucomannan, but this value has never been used to predict the cell wall elastic constants.

In this paper, the elastic constants of the wood cell wall

layers were calculated using the unit models proposed by Tang et al., Ohgama et al. and Norimoto et al.. Three different sets of elastic constants of matrix were adopted in the calculation. Further, the elastic constants for two types of the cell wall models as a function of the microfibril angle of the S_2 layer were calculated to investigate the influence of cell wall unit models and elastic constants of matrix on the elastic behavior of the cell wall. The results obtained were compared with experimental data reported.

2. Analysis of Elastic Constants of Cell Wall Models

2.1 Cell wall unit models

Figure 1a shows one of the unit models of the cell wall layer (Type-A)[3,4]. In this model, an anisotropic framework of crystalline cellulose (region F) is surrounded by an isotropic lignin-hemicellulose matrix (region M). Its cross section was assumed to be square. Table 1 shows the elastic constants of framework and matrix as well as their volume fractions in each cell wall layer. I, P and S represent the intercellular layer, primary wall and secondary wall, respectively. As the elastic constants in region F, both experimental and estimated values of crystalline cellulose[4,9,10] were adopted. Three different sets of elastic constants for the matrix were used. The
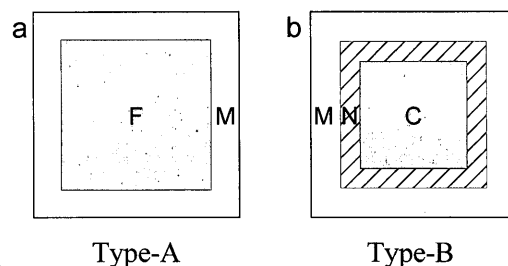

Type-A   Type-B

Fig. 1. Cross sections of cell wall unit models. a : Type-A unit model[3,4], b : Type-B unit model[5]. F : framework, M : matrix, C : crystalline cellulose, N : non-crystalline cellulose.

[*1] Laboratory of Property Enhancement.
[*1] Present address: Material Structural Formation Process Department, National Industrial Research Institute of Nagoya, Hirate-cho, Kita-ku, Nagoya 462-8510, Japan.

Table 1a. Volume fractions of framework and matrix in Type-A cell wall layers.

Cell wall layer	I+P	S_1	S_2	S_3
Framework	0.10	0.53	0.53	0.53
Matrix	0.90	0.47	0.47	0.47

I : intercellular layer, P : primary wall, S : secondary wall.

Table 1b. Elastic constants of framework and matrix in Type-A cell wall layers.

Elastic constants	E_x	$E_y = E_z$	G_{yz}	$G_{zx} = G_{xy}$	ν_{yz}	ν_{zx}	ν_{xy}
Framework	134	27.2	13.0	4.40	0.04	0.02	0.10
Matrix 1	2.00	2.00	0.77	0.77	0.30	0.30	0.30
Matrix 2	4.00	4.00	1.50	1.50	0.30	0.30	0.30
Matrix 3	6.00	6.00	2.30	2.30	0.30	0.30	0.30

E (GPa) : directional Young's modulus, G (GPa) : shear modulus, ν : Poisson's ratio, x : direction parallel to microfibril length, y and z : direction perpendicular to x.

Table 2a. Volume fractions of regions C, N and M in Type-B cell wall layers.

Cell wall layer	I+P	S_1	S_2	S_3
Region C	0.13	0.22	0.27	0.16
Region N	0.12	0.19	0.24	0.14
Region M	0.75	0.59	0.49	0.70

I : intercellular layer, P : primary wall, S : secondary wall.

Table 2b. Elastic constants of crystalline and noncrystalline celluloses and matrix in Type-B cell wall layers.

Elastic constants	E_x	$E_y = E_z$	G_{yz}	$G_{zx} = G_{xy}$	ν_{yz}	ν_{zx}	ν_{xy}
Crystalline cellulose	134	27.2	13.0	4.40	0.04	0.02	0.10
Noncrystalline cellulose	110	22.3	10.7	3.61	0.04	0.02	0.10
Matrix 1	2.00	2.00	0.77	0.77	0.30	0.30	0.30
Matrix 2	4.00	4.00	1.50	1.50	0.30	0.30	0.30
Matrix 3	6.00	6.00	2.30	2.30	0.30	0.30	0.30

E (GPa) : directional Young's modulus, G (GPa) : shear modulus, ν : Poisson's ratio, x : direction parallel to microfibril length, y and z : direction perpendicular to x.
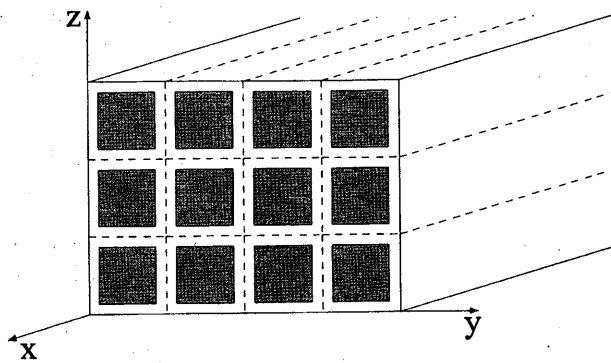

Fig. 2. Cell wall layer and its elastic coordinates. x : direction parallel to microfibril length, y and z : direction perpendicular to x.

Table 3. Volume fractions and mirofibril angles of cell wall layars.

Cell wall layer	I+P	S_1	S_1	S_2	S_3
Volume fraction	0.07	0.04	0.04	0.80	0.05
Microfibril angle (°)	90	67	−67	0–45	82

I : intercellular layar, P : primary wall, S : secondary wall.
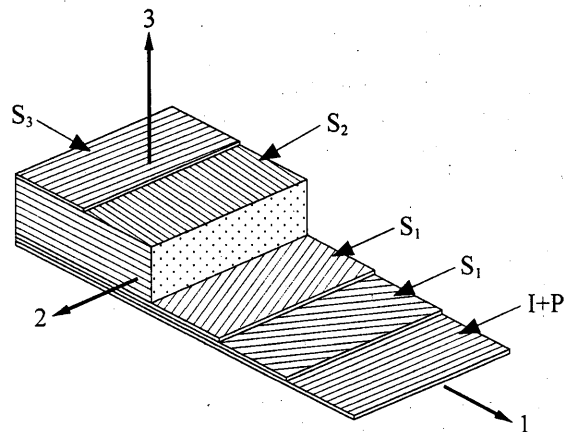

Fig. 3. Single cell wall model and its elastic coordinates. I : intercellular layer, P : primary wall : S : secondary wall, 1 : longitudinal direction, 2 : perimetric direction, 3 : thickness direction.

elastic constants of Matrix 1 and 2 in Table 1b were calculated using the experimental Young's moduli of 2 and 4 GPa obtained for isolated lignin, respectively. The value of the Young's modulus in Matrix 3, 6 GPa, was

Table 4a. Calculated elastic constants of Type-A cell wall layers.

Elastic constants	Matrix 1		Matrix 2		Matrix 3	
	I+P	S	I+P	S	I+P	S
E_x	15.3	72.2	17.2	73.1	19.0	74.1
E_y	2.62	6.25	5.04	10.5	7.33	13.6
E_z	3.05	7.13	5.56	11.4	7.81	14.3
G_{yz}	0.85	1.54	1.65	2.83	2.51	4.09
G_{zx}	0.95	1.77	1.71	2.62	2.48	3.25
G_{xy}	0.86	1.62	1.63	2.51	2.43	3.19
ν_{zy}	0.31	0.15	0.32	0.18	0.32	0.19
ν_{zx}	0.05	0.02	0.08	0.03	0.11	0.03
ν_{xz}	0.29	0.19	0.29	0.19	0.29	0.19

I : intercellular layer, P : primary wall, S : secondary wall, E (GPa) : directional Young's modulus, G (GPa) : shear modulus, ν : Poisson's ratio, x : direction parallel to microfibril length, y and z : direction perpendicular to x.

Table 4b. Calculated elastic constants of Type-B cell wall layers.

Elastic constants	Matrix 1				Matrix 2				Matrix 3			
	I+P	S_1	S_2	S_3	I+P	S_1	S_2	S_3	I+P	S_1	S_2	S_3
E_x	32.2	51.9	63.3	37.6	33.8	53.1	64.3	39.0	35.3	54.3	65.3	40.4
E_y	3.46	4.77	5.81	3.76	6.40	8.34	9.74	6.87	8.99	11.2	12.7	9.54
E_z	4.13	5.58	6.64	4.49	7.16	9.19	10.6	7.67	9.64	11.9	13.3	10.2
G_{yz}	1.01	1.25	1.46	1.06	1.92	2.35	2.69	2.02	2.88	3.45	3.89	3.01
G_{zx}	1.17	1.45	1.65	1.24	1.94	2.25	2.45	2.02	2.66	2.91	3.05	2.73
G_{xy}	1.03	1.30	1.51	1.10	1.84	2.15	2.36	1.92	2.61	2.86	3.01	2.67
ν_{yz}	0.25	0.19	0.16	0.23	0.27	0.21	0.19	0.25	0.28	0.23	0.20	0.27
ν_{zx}	0.03	0.02	0.02	0.02	0.05	0.03	0.03	0.04	0.06	0.04	0.04	0.06
ν_{xy}	0.26	0.22	0.19	0.25	0.26	0.22	0.19	0.25	0.26	0.22	0.20	0.25

I : intercellular layer, P : primary wall, S : secondary wall, E (GPa) : directional Young's modules, G (GPa) : shear modulus, ν : Poisson's ratio, x : direction parallel to microfibril length, y and z : direction perpendicular to x.
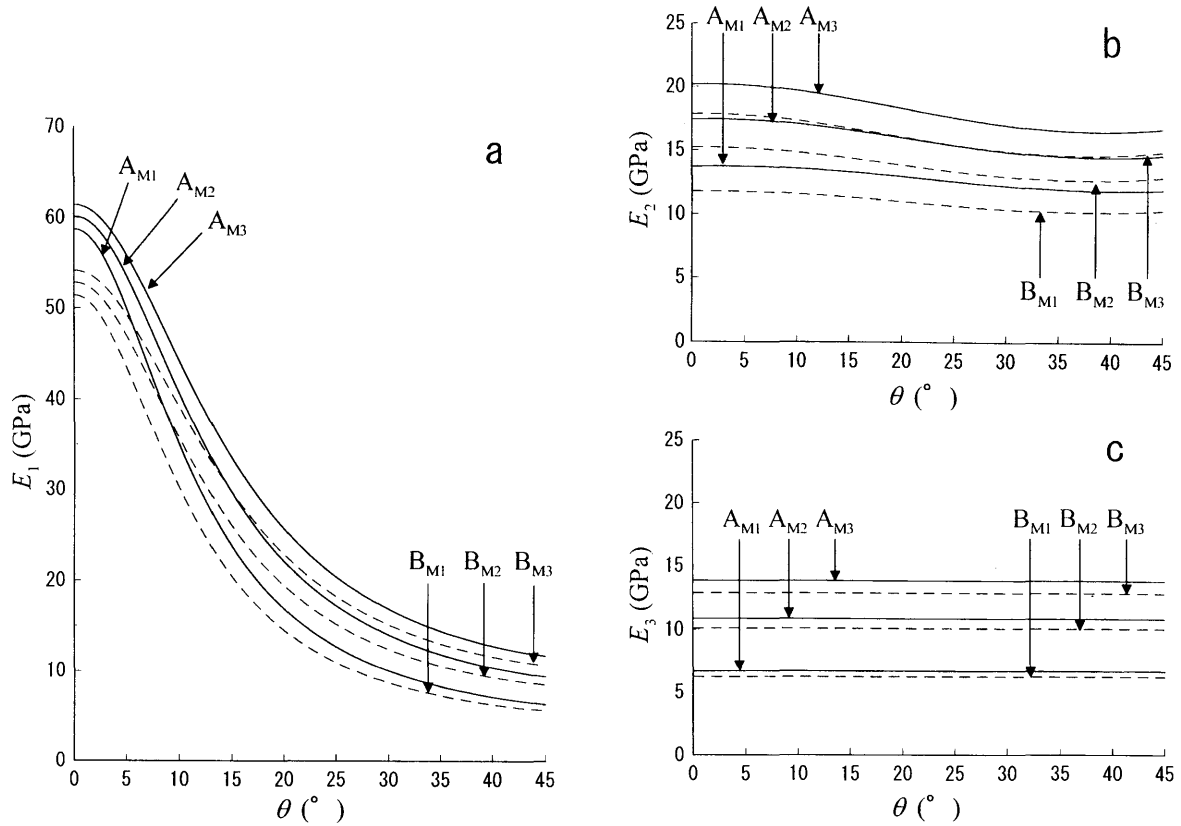

Fig. 4. Calculated Young's moduli of cell wall models E_1, E_2 and E_3 as a function of microfibril angle of the S_2 layer θ. A : Type-A cell wall model, B : Type-B cell wall model, M1 : Matrix 1, M2 : Matrix 2, M3 : Matrix 3.

obtained assuming that the matrix consisted of equal volume fractions of isotropic hemicellulose and isotropic lignin and they had the Young's moduli of 8 and 4 GPa, respectively.

Another unit model[5] is shown in Fig. 1b (Type-B). In this model, crystalline cellulose (region C) is surrounded by non-crystalline cellulose (region N) and an isotropic lignin-hemicellulose matrix (region M). Its cross section was also assumed to be square. Table 2 shows the elastic constants of each region and their volume fraction in each cell wall layer. The elastic constants in region N were calculated with reference to a directional Young's modulus of 110 GPa predicted by Norimoto[11]. The elastic constants of matrix used in the Type-A unit model were also adopted in region M of the Type-B unit model.

2.2 Three dimensional analysis of cell wall models

The unit model repeatedly produces the cell wall layer

shown in Fig. 2. The Young's moduli E_i (i=x, y, z), shear moduli G_{ij} (i, j=x, y, z, i≠j) and Poisson's ratios ν_{ij} (i, j=x, y, z, i≠j) of cell wall layers were evaluated by using the formulas for the elastic constants of three dimensional layered media derived by Chou et al.[12]. In the calculation, it was assumed that the normal strains in the element parallel to the layers and the shear strain in the plane of the layers are uniform and the same for each ingredient, and that the normal stress perpendicular to the layers and the shear stresses in the planes perpendicular to the layers are uniform and the same in each material. Both equilibrium at the interface and the compatibility of the material were satisfied by these assumptions. The Young's moduli E_k (k=1, 2, 3), shear moduli G_{kl} (k, l=1, 2, 3, k≠l) and Poisson's ratios ν_{kl} (k, l=1, 2, 3, k≠l) of single cell wall models shown in Fig. 3 were evaluated by the same procedure. Table 3 shows the volume fractions and microfibril angles in all layers. Further, the bending
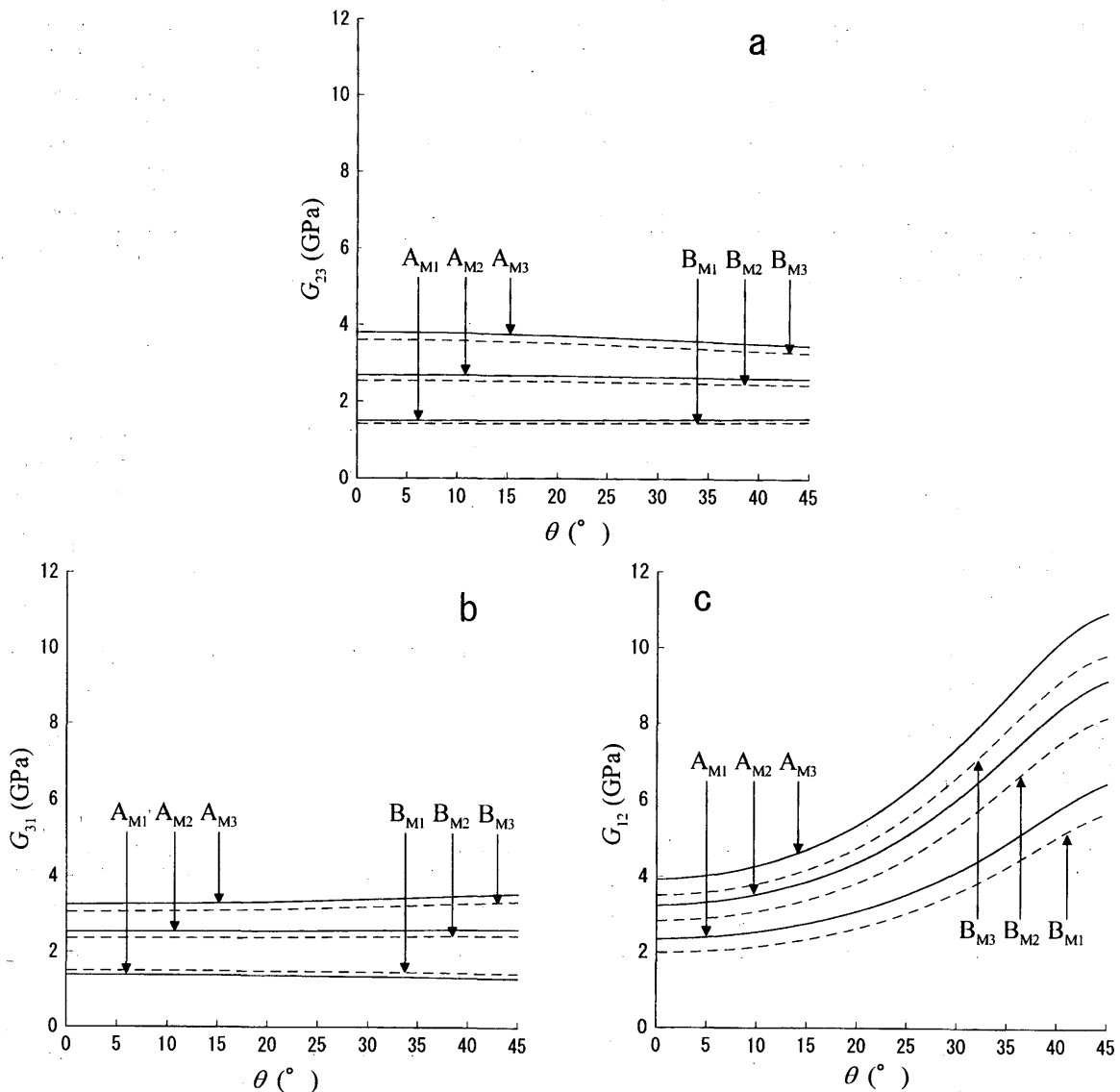

Fig. 5. Calculated shear moduli of cell wall models G_{23}, G_{31} and G_{12} as a function of microfibril angle of the S2 layer θ. A: Type-A cell wall model, B: Type-B cell wall model, M1: Matrix 1, M2: Matrix 2, M3: Matrix 3.

elastic modulus of double cell wall models in 2-direction E_{b2} were analyzed by means of the lamination theory[13]. It is considered that E_{b2} is an important constant in analyzing the transverse Young's modulus of wood in relation to cell shape.

3. Result and Discussion

3.1 Elastic constants of cell wall layers

Table 4a shows the calculated elastic contants of Type-A cell wall layers. The $E_{y,z}$ and G_{ij} for both I+P and S layers increased remarkably with increasing E and G of matrix, although the E_x and ν_{ij} didn't change significantly. Table 4b shows the calculated elastic constants of Type-B cell wall layers. As in the results of Type-A cell wall layers, the $E_{y,z}$ and G_{ij} for all layers increased remarkably with increasing E and G of matrix. From the large volume fraction of cellulose with high Young's modulus and shear modulus in the Type-B I+P layer, the E and G

for the Type-B I+P layer were larger than those for the Type-A I+P layer. On the other hand, the E and G for each Type-B S layer were smaller than those for the Type-A S layer. This result was due to the small volume fraction of cellulose and the existence of non-crystalline cellulose with small Young's modulus and shear modulus in each Type-B S layer. The ν for the Type-B I+P layer was slightly smaller than that for the Type-A I+P layer, whereas the ν for the Type-B S layer was slightly larger than that for the Type-A S layer. Among Type-B S layers, the Young's modulus and shear modulus decreased while the Poisson's ratios increased, in the order of the S_2, S_1, and S_3 layers, which corresponded to the volume fractions of cellulose.

3.2 Elastic constants of the cell wall and microfibril angle of the S₂ layer

Figure 4 shows the calculated Young's moduli of the cell wall models E_1, E_2 and E_3 as a function of microfibril angle
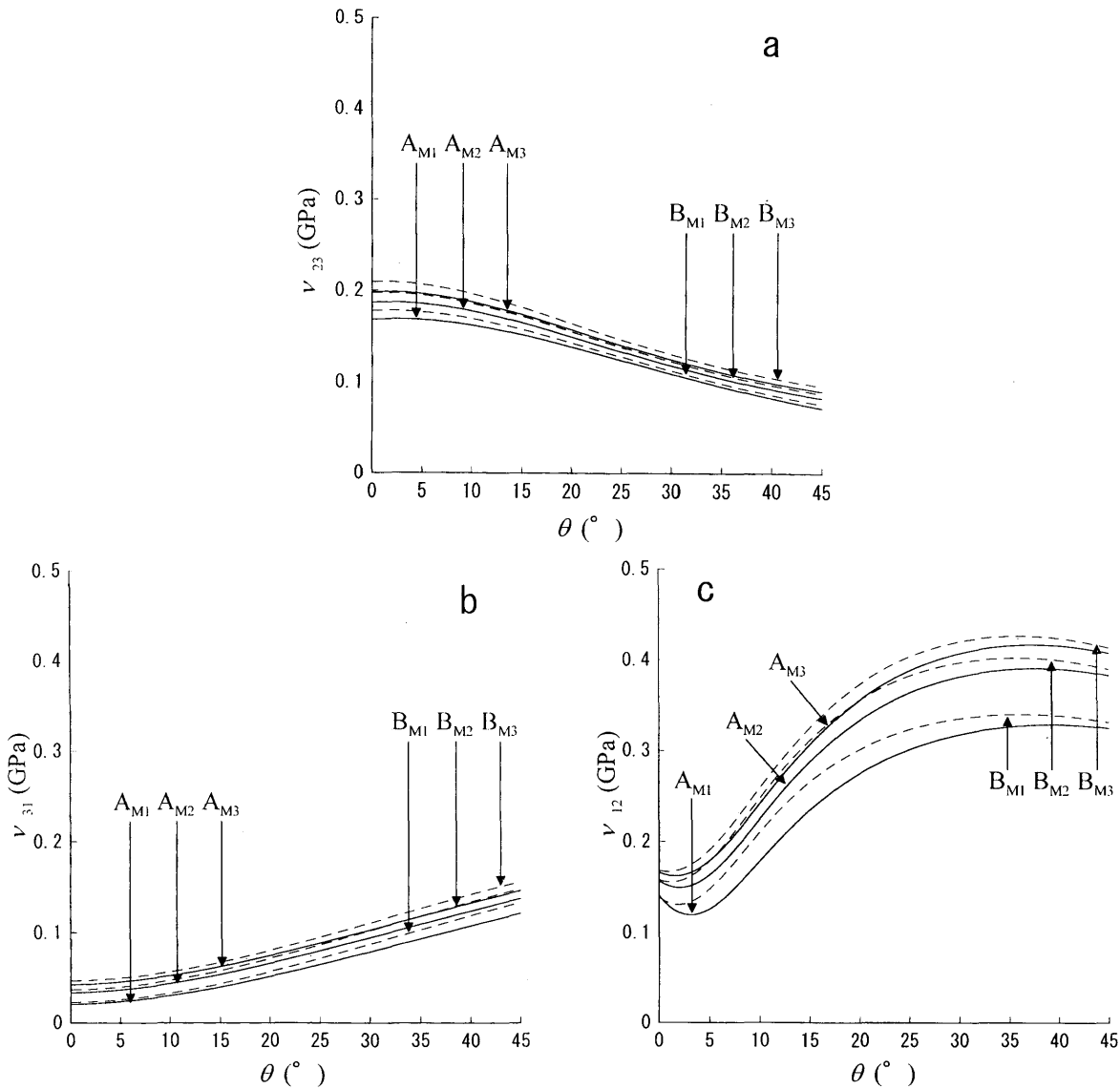

Fig. 6 Calculated Poisson's ratios of cell wall models ν_{23}, ν_{31} and ν_{12} as a function of microfibril angle of the S_2 layer θ. A : Type-A cell wall model, B : Type-B cell wall model, M1 : Matrix 1, M2 : Matrix 2, M3 : Matrix 3.

of the S_2 layer θ. The E_1 and E_2 of the Type-B model were smaller than those of the Type-A model. These results were attributed to the small volume fraction of cellulose and the existence of non-crystalline cellulose in the Type-B S layers. The E_3 of the Type-B model was also smaller than that of the Type-A model, but the difference was not significant. For both Type-A and Type-B models, the highest Young's moduli were obtained when the elastic constants of Matrix 3 in Table 1 were adopted. The E_1 decreased steeply with increasing θ, in the range of θ from 4° to 25°, and decreased gently above $\theta=25°$. The decrease of E_1 with θ became more gentle with increasing E and G of matrix. It was considered that the variation of E_y and G_{xy} with the elastic constants of matrix related to the decrease of E_1 with θ, because the E_x for the cell wall layers among the three different matrix types shown in Table 4 didn't differ largely. The E_2 decreased slightly with θ and increased slightly above about $\theta = 40°$. The calculated results of E_3 were independent of θ, but depended on the elastic constants of matrix.

Figure 5 shows the calculated shear moduli of the cell wall models G_{23}, G_{31} and G_{12}. The highest shear moduli for both Type-A and Type-B models were obtained when the elastic constants of Matrix 3 were adopted, although the calculated values of the Type-B model were slightly smaller than those of the Type-A model except the result of G_{31} calculated using Matrix 1. With increasing θ, the G_{23} and G_{31} remained almost unchanged, but the G_{12} increased, especially above $\theta=20°$.

Figure 6 shows the calculated Poisson's ratios of the cell wall models ν_{23}, ν_{31} and ν_{12}. The highest Poisson's ratios for both Type-A and Type-B models were obtained when the elastic constants of Matrix 3 were adopted. With increasing θ, the ν_{23} gently decreased and the ν_{31} increased. There was almost no difference in the

calculated result of the ν_{23} or the ν_{31} between Type-A and Type-B models. With increasing θ the ν_{12} slightly decreased in the range of θ from 0° to 3° and then increased remarkably.

Figure 7 shows the calculated bending elastic moduli of the cell wall models in 2-direction E_{b2}. The highest modulus was obtained for each model when the elastic constants of Matrix 3 were used. The E_{b2} varied gently with θ. The bending behavior perpendicular to thickness direction for layered media depends strongly on the mechanical property of the laminated material at the outermost layer. Both the elastic constants on the 1–2 plane and the volume fraction of the S_3 layer contributed to the calculated E_{b2}. Therefore, the parameter θ didn't influence significantly the calculated E_{b2} in the range of θ from 0° to 45°. The smaller calculated value for Type-B than Type-A model was related to the small volume fraction of cellulose and the existence of non-crystalline cellulose in the Type-B unit model.

3.3 Comparison between calculated and experimental results for E_1, E_2 and E_{b2}

Norimoto et al.[14] and Sobue et al.[15] reported experimental values for the longitudinal Young's modulus of coniferous wood cell wall. Figure 8 shows a comparison of the calculated and experimental results. The calculated values of E_1 for the Type-A model (solid lines) were larger than the experimental ones for $\theta < 10°$, and the calculated values of E_1 for Type-B (dotted lines) almost coincided with the experimental values. Since high E and
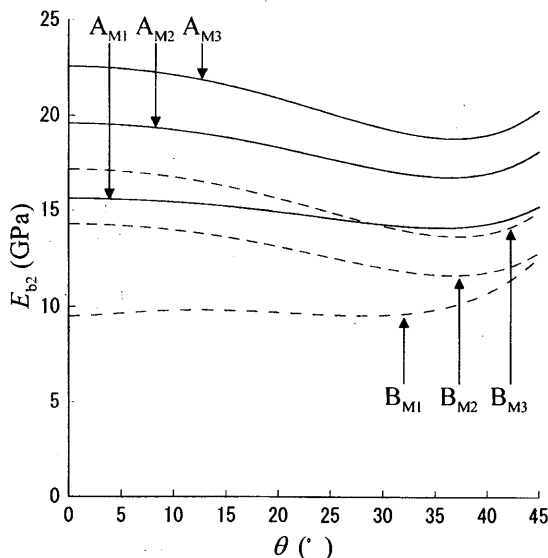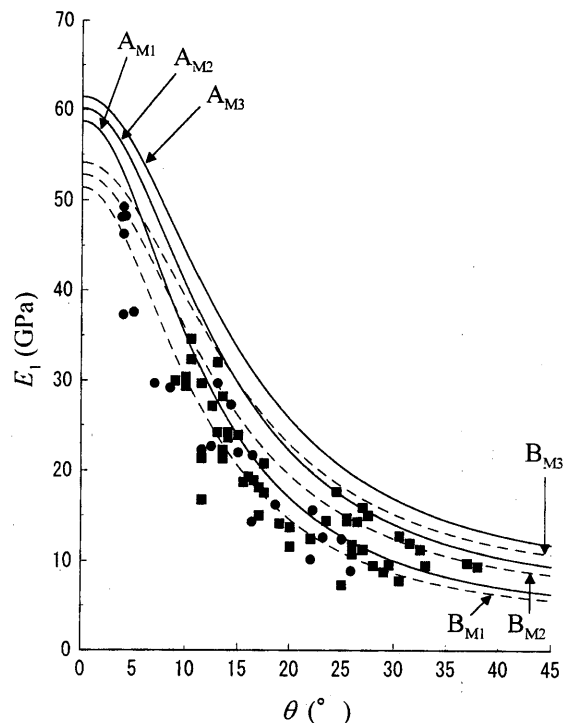
Fig. 7. Calculated elastic bending moduli in 2-direction of cell wall models E_{b2} as a function of microfibril angle of the S_2 layer θ. A : Type-A cell wall model, B : Type-B cell wall model, M1 : Matrix 1, M2 : Matrix 2, M3 : Matrix 3.

Fig. 8. Comparison between experimental and calculated results for E_1. Symbols ● and ■ represent the experimental data in Norimoto et al.[14] and Sobue et al.[15], respectively. A : Type-A cell wall model, B : Type-B cell wall model, M1 : Matrix 1, M2 : Matrix 2, M3 : Matrix 3.
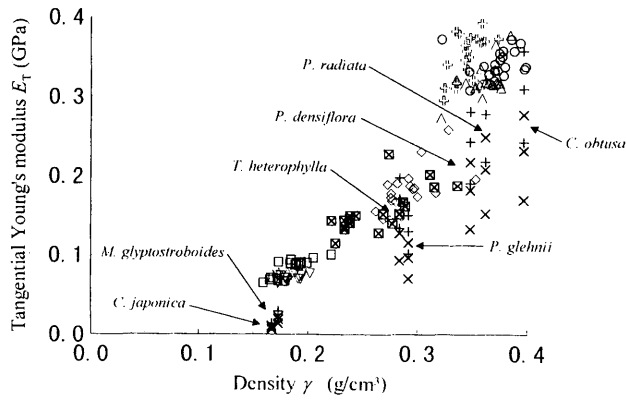
Fig. 9. Comparison between experimental and calculated results of tangential Young's modulus $E_T^{16)}$. $\square$: *Cryptomeria japonica*, $\bigcirc$: *Chamaecyparis obtusa*, $\Diamond$: *Picea glehnii*, $\oplus$: *Pinus densiflora*, $\triangle$: *Pinus radiata*, ∇: *Metasequoia glyptostroboides*, $\boxtimes$: *Tsuga heterophylla*, +: calculated with Type-A model elastic constants, ×: calculated with Type-B model elastic constants.

G were used for the framework, the resultant calculated value of E_1 was obtained for the Type-A model. These results may indicate that the adopted volume fraction and elastic constants for non-crystalline cellulose shown in Table 2b are reasonable. The E_1 calculated with the elastic constants of Matrix 1 in Table 1 were smaller than the experimental values. In the range of θ from 4° to 25°, the E_1 calculated using the elastic constants of Matrix 1 seemed to fall steeply compared with experimental results. With increasing E and G of matrix, the change of E_1 with θ became gentle, which corresponded to the experimental trends. Both the E_2 and E_{b2} are important when analyzing the transverse Young's modulus of wood in relation to the cellular structure. In Fig. 9, the tangential Young's moduli E_T of coniferous early wood cell models[16] calculated using the E_2 and E_{b2} obtained were compared

with the experimental results. The calculated values of E_T at $\theta=6°$ increased with increasing E and G of matrix. The values calculated using the highest E_2 and E_{b2} for the Type-A model with Matrix 3 agreed well with the experimental ones. The values calculated using the lowest E_2 and E_{b2} for the Type-B model with Matrix 1 were much lower than the experimental values. These results indicate that the wood cell wall would contain a non-crystalline cellulose with lower elastic moduli than crystalline cellulose and the Young's modulus of the lignin-hemicellulose matrix is at least more than 2 GPa.

References

1) R. Wimmer *et al.*: *Wood Sci. Technol.*, **31**, 131–141 (1997).
2) R. Wimmer and B.N. Lucas: *IAWA*, **18**(1), 77–88 (1997).
3) R.C. Tang and N.N. Hsu: *Wood and Fiber*, **5**(2), 139–151 (1973).
4) T. Ohgama and M. Norimoto: *Bull. Fac. Edu., Chiba Univ.*, **33**, 127–145 (1984).
5) M. Norimoto and K. Takabe: *Wood Res. Tech. Notes*, **21**, 96–101 (1985).
6) P.S. Srinivasan: *Quart. J. Indian Inst. Sci.*, **4**(2), 222–314 (1941).
7) W.J. Cousins: *Wood Sci. Technol.*, **10**, 9–17 (1976).
8) W.J. Cousins: *Wood Sci. Technol.*, **12**, 161–167 (1978).
9) I. Sakurada *et al.*: *J. Polymer Sci.*, **57**, 651–660 (1962).
10) R.E. Mark: "Cell Wall Mechanics of Tracheids", Yale Univ. Press, New Heaven and London, pp. 119 (1967).
11) M. Norimoto: "Construction of New Cellulose Microfibril Model (T. Okano ed.)", Report of a Grant-in-Aid for Scientific Research (No. 08306009) from The Ministry of Education, Science and Culture (1999).
12) P.C. Chou *et al.*: *J. Comp. Mater.*, **6**, 80–93 (1972).
13) R.M. Jones: "Mechanics of Composite Materials (International student edition)", McGraw-Hill Kogakusha, Tokyo, pp. 147–237 (1975).
14) M. Norimoto *et al.*: *Wood Res. Tech. Notes*, **22**, 53–65 (1986).
15) N. Sobue and I. Asano: *Mokuzai Gakkaishi*, **22**(4), 211–216 (1976).
16) U. Watanabe *et al.*: *Holzforschung*, **53**, 209–214 (1999).